Computer Simulation and Theory for Free Energies in Dilute Near-Critical Solutions

T. W. Li, F. Munoz, and E. H. Chimowitz
Dept. of Chemical Engineering, University of Rochester, Rochester, NY 14627

Computer simulation results are presented for the residual chemical potential μ_1^r, local solvent density enhancement $\Delta\rho_{loc}$, and average solute potential energy u_1 of a solute molecule immersed in a fluid very close to its critical point. The simulation algorithm involves the Monte Carlo method in conjunction with free energy perturbation ideas. A number of ideas related to the feasibility of computer simulations in near-critical solvents are investigated. Due to long-range correlations near the critical point, it is not clear that simulations in this regime can be expected to yield accurate results using ensemble sizes of the magnitude typically used in simulations. Examination of system size and number of sampling steps on the simulations shows that the accuracy of the results depend to a large extent on the nature of the thermodynamic property being investigated. The solute chemical potential is suited particularly to simulation since it depends primarily on short-range structure in the system. A comparison of the simulation results with integral equation theory calculations shows both approaches agree well with each other.

Introduction

Fluids near their critical points exhibit large compressibility changes and other unusual solution behavior. Some of these effects have been proposed as the basis for new separations technology involving the use of supercritical fluid solvents. To better understand solvation thermodynamics in near-critical solutions, statistical mechanical theories of fluid behavior have often been used either in the form of integral equation theories (McGuigan and Monson, 1990; Wu et al., 1990; Munoz and Chimowitz, 1992) and/or computer simulation methods (Vogelsang and Hoheisel, 1984; Shing and Chung, 1987, 1988; Petsche and Debenedetti, 1989; Nouacer and Shing, 1989). Although Monte Carlo (MC) and Molecular dynamic (MD) simulation methods provide powerful techniques for investigating solvation thermodynamics in these systems, the accuracy of simulation results for systems very near their critical points is still a debatable issue. There are a number of reasons for this; an important one is being the use of periodic boundary conditions for constructing infinite images in conventional MC or MD simulations. Long-range density fluctuations near the gas-liquid critical point, specifically those with wavelengths greater than the length of the sampling box L, are suppressed artificially through this simulation construct. In this situation, there is a dilemma associated with the simulation of a system using small sample sizes of the magnitude typically used in simulations. Can we achieve reasonable results in these situations and if so, for what classes of thermodynamic properties? These are essentially the points we address in this article using a Monte Carlo algorithm in conjunction with free energy perturbation theory to carry out the simulations.

Shing and Gubbins (1981, 1982) provided some notable early simulation results for the calculation of chemical potentials in Lennard-Jones mixtures at high densities using a MC method. In subsequent work, Shing and Chung (1987) argued that the isothermal-isobaric (NPT) ensemble was particularly convenient to use for supercritical fluids since it explicitly permitted density fluctuations. Those authors used MC simulations with both the test particle method based on Widom's potential distribution theorem (1963), and the Kirkwood coupling method (McQuarrie, 1973) for calculating the residual chemical potential μ_1^r of a solute immersed in a supercritical fluid solvent. At low to moderate pressures, both methods essentially gave similar results; however, at high pressure the Kirkwood coupling method proved to be more accurate and stable. It is well established that the test particle method fails at high densities

because of its inability to sample favorable configurations (Panagiotopoulos et al., 1986). Shing and Chung also compared their simulation results to experimental solubility data for the CO_2/Naphthalene system and concluded that the significant discrepancies observed between the simulation results and the experimental data were a consequence of the crude nature of the CO_2 potential used. This particular potential was of the Lennard-Jones form with a quadrupole moment term, and had been fit to experimental saturated vapor-liquid density data for CO_2.

In another study using Lennard-Jones mixtures, Shing and Chung (1988) calculated a wider range of thermodynamic properties in addition to the solute residual chemical potential μ_1^r. These included the solute partial molar internal energy $\overline{U}_1^\infty$ and its partial molar volume counterpart $\overline{V}_1^\infty$, at the limit of infinite dilution in the NPT ensemble. The infinite dilution limit is considered to be a useful reference condition for analyzing dilute supercritical mixture behavior. There appeared to be significant differences in the statistical accuracy of the simulation results for these two property types. The results for μ_1^r showed relatively small fluctuations about their mean values, while the fluctuations in the other two properties were extremely large. For example, in a system of Lennard-Jones molecules (with potential parameters $\epsilon_{12}=0.5\epsilon_{22}$, $\sigma_{12}^3=3.5\sigma_{22}^3$, $T^*=1.5$, $\rho^*=0.3$), the simulation results for $\overline{U}_1^\infty$ were given as -0.4 ± 10 and $\overline{V}_1^\infty=24.7\pm18$ ($\overline{U}_1^\infty$ was reduced with respect to ϵ_{22} and $\overline{V}_1^\infty$ with respect to σ_{22}^3). In this notation, 1 refers to the solute species, 2 the solvent, ϵ is the well-depth parameter, σ the molecular diameter term and T^* and ρ^* the reduced temperature and density of the Lennard-Jones system defined as $T^*=kT/\epsilon_{22}$, $\rho^*=N\sigma_{22}^3/V$. We believe that the large uncertainties associated with the simulation results for these latter properties is directly related to the issue of long-range correlations and the problems they may present for computer simulation in dilute near-critical mixtures, a focus of this work.

A distinction between short and long-range effects affecting solvation in a near-critical solvent was explicitly considered by Munoz and Chimowitz (1992) who showed that the diverging parts of the solute residual partial molar entropy and its energetic counterpart cancel exactly. As a result, these divergent terms *do not* contribute in determining the value of the solute's residual chemical potential in solution. Since this divergent behavior is related to long-range effects, this result implies that the solute chemical potential is representative of short-range structural adaptations in the fluid. In this sense, the chemical potential is an ideal property for study with computer simulation, regardless of the ensemble type used and/or proximity to the solvent critical point. The extent of the so-called short-range neighborhood, responsible for the dominant contribution to μ_1^r, was investigated by Munoz and Chimowitz using integral equation theory calculations. They consistently found this neighborhood to be a spatial domain of approximately three solvent diameters around the solute molecule, independent of the extent of density fluctuations in the system. The solute's partial molar internal energy $\overline{U}_1^\infty$ and its volumetric counterpart $\overline{V}_1^\infty$, however, intrinsically involve long-range correlations and remain more difficult quantities to determine with small sample sizes especially when near the critical point. Towards this end, Munoz and Chimowitz defined two new short-range properties related to the solute's free energy of solvation, namely the average solute potential *energy* denoted by u_1, and the solute's local *entropy* of solvation denoted by s_1^r. In addition to being informative about solution behavior, it is shown here that these properties can be calculated using MC simulation methods with small sample sizes near the mixture critical point. The investigation of these and other issues is taken up in this article. We explicitly study the system at, or extremely close to its accepted critical point. Previously reported simulation results in dilute supercritical mixtures have by comparison been at conditions much more removed from the critical point itself. In addition, we often provide comparisons between the simulation results and integral equation theory calculations of the sort described in Munoz and Chimowitz. Those calculations used the Kirkwood-Buff formalism (1951) in conjunction with the PY (Percus-Yevick, 1958) equation for the mixture pair correlation functions. While this is an approximate classical theory, it is widely used, and closely satisfies important thermodynamic consistency properties at near-critical conditions (Munoz and Chimowitz, 1992).

Theoretical Background to the Simulations

A common feature of computer simulation is the use of small molecular aggregates to calculate average thermodynamic properties for a macroscopic system where this average is taken according to some prescribed statistical distribution, for example, the Boltzmann distribution. These averaged values correspond to the mean property value in the macroscopic system. This presents a potential dilemma if the system being simulated is near a critical point, because of long-range correlations intrinsic to this region. Implicit to this point is the notion that in this region thermodynamic properties depend upon averages taken over macroscopic dimensions. This may complicate the use of simulation methods in these systems and is one of the points we address, particularly with reference to the solute chemical potential when solvated in a solvent near its critical point.

Consider a binary solution of a solute (species 1) in a solvent (species 2). In the limit of infinite dilution when $x_1\to0$, the residual chemical potential of the solute derived by the Kirkwood coupling approach (McQuarrie, 1973) can be expressed as:

$$\mu_1^r=\rho\int_0^1\int_0^\infty u_{12}(r)g_{12}(r,\xi)4\pi r^2dr d\xi \tag{1}$$

where $u_{12}(r)$ is the intermolecular potential between solute 1 and solvent 2, ξ is the Kirkwood coupling parameter, ρ the phase density and $g(r,\xi)$ the pair correlation function with the system coupled to the extent ξ. A thermodynamic definition for the property μ_1^r can be given as:

$$\mu_1^r=\overline{H}_1^r-T\overline{S}_1^r \tag{2}$$

where $\overline{H}_1^r$ is the residual partial molar enthalpy of the solute, $\overline{S}_1^r$ its partial molar entropy and T the temperature. In their article, Munoz and Chimowitz (1992) proved that the long-range contributions to both the energetic and entropic terms in the righthand side of Eq. 2 cancel exactly. A consequence of this result is that μ_1^r is predominantly given by short-range effects, independent of whether or not the solvent is near its critical point. This result may also be anticipated from Eq. 1

where the intermolecular potential term in the integrand will tend to dampen long-range effects that show up in the pair correlation function as the solvent approaches criticality. Self-consistent definitions for these short-range energetic and entropic effects that contribute to μ_1^r were proposed by these authors and are given as:

$$u_1 = \rho \int_0^\infty u_{12}(r) g_{12}(r, \xi = 1) 4\pi r^2 dr \tag{3}$$

$$s_1^r = \frac{u_1 - \mu_1^r}{T} \tag{4}$$

where μ_1^r is given by Eq. 1. It should be stressed that the functions u_1 and s_1^r are *not* the usual energetic and entropic properties commonly used in the equation defining the chemical potential. In particular,

$$u_1 \neq \left(\frac{\partial U}{\partial N_1}\right)_{T,V,N_2} \tag{5}$$

and

$$s_1^r \neq \left(\frac{\partial S^r}{\partial N_1}\right)_{T,V,N_2} \tag{6}$$

Furthermore, $u_1 \neq \overline{U}_1$ and $s_1^r \neq \overline{S}_1^r$, where $\overline{U}_1$ and $\overline{S}_1^r$ are the respective partial molar properties of the solute in solution.

The spatial dependence of the solute chemical potential and its decomposition into energetic and entropic contributions as defined by Eqs. 3 and 4 above can be investigated by studying a function $F_{12}(R)$ defined as:

$$F_{12}(R) = \rho \int_0^R \int_0^1 u_{12}(r) g_{12}(r, \xi) 4\pi r^2 d\xi dr \tag{7}$$

From this definition for $F_{12}(R)$,

$$\lim_{R \to \infty} F_{12}(R) = \mu_1^r \tag{8}$$

Obviously, the idea that μ_1^r is given by short-range effects implies that the limit $R \to \infty$ in Eq. 8, while an exact result, is much too conservative a criterion. A question naturally arises as to the value of R that defines the neighborhood primarily responsible for setting a value for μ_1^r, a point taken up by Munoz and Chimowitz (1992). Their results consistently demonstrated that the spatial domain predominantly responsible for establishing a value for μ_1^r was a small neighborhood (corresponding to approximately three solvent molecular diameters) around the solute species. This appeared to be the case irrespective of the proximity to the solvent critical point. From these results we may conclude that the solute chemical potential, besides being an important property for describing solvation thermodynamics, is also an ideal property from the perspective of computer simulation studies in near-critical fluids.

Table 1. Lennard-Jones Potential Parameters for the System

	Solvent-Solvent	Solvent-Solute	Solute-Solute
ϵ_{ij}/k (K)	204.68	353.20	629.45
σ_{ij} (Å)	3.831	4.729	5.627

Simulation Method

We chose to study a Lennard-Jones system with parameters corresponding to those in Table 1 which will allow us to compare the simulation results with the integral equation theory calculations. The parameters in Table 1 correspond to a situation where the solute is larger than the solvent species and is representative of most real systems of interest in supercritical fluid technology. Since this study was primarily concerned with developing and testing simulation methods rather than attempting to examine quantitative agreement with experimental data, no attempt was made to optimize the potentials.

Free-energy perturbation method

Consider a binary solution of a solute (species 1) in a solvent (species 2). The residual chemical potential μ_1^r of solute 1 is:

$$\mu_1^r = \left(\frac{\partial A^r}{\partial N_1}\right)_{T,V,N_2} \tag{9}$$

where μ_1^r can be explicitly written as:

$$\mu_1^r = A^r(T, V, N_2, N_1) - A^r(T, V, N_2, N_1 - 1) \tag{10}$$

For an infinite-dilute solution, N_1 is set to be 1 and Eq. 9 becomes:

$$\mu_1^r = A^r(T, V, N_2, N_1 = 1) - A^r(T, V, N_2, N_1 = 0) \tag{11}$$

From perturbation theory (Widom, 1963; Jorgensen and Ravimohan, 1985), Eq. 9 can be represented as:

$$\mu_1^r = A_1^r - A_{II}^r = -kT \ln \langle \exp[-\beta(u_1 - u_{II})] \rangle_{II} \tag{12}$$

where k is the Boltzmann constant, T is the absolute temperature, $\beta = 1/kT$, u_i is the intermolecular potential energy in state i (state I represents N_2 solvent molecules with 1 solute; state II represents N_2 solvent molecules). The configuration ensemble average $\langle \ \rangle_{II}$ is taken with respect to reference state II. Unless the two fluids are very similar implying that $\beta(u_1 - u_{II})$ is small for all the important configurations in the ensemble, the average in Eq. 12 is difficult to calculate accurately (Allen and Tildesley, 1987). A way to compensate for this potential problem is to define a coupling parameter λ that allows the perturbation to be turned on gradually (Singh et al., 1987). As a result, the computational implementation of Eq. 10 is as follows. If the two systems differ significantly as is the case here, the states between II and I are defined through a perturbation parameter λ as:

$$u_\lambda = \psi_1(\lambda) + \sum_{i=1}^{N-1} \sum_{j=i+1}^{N} u_{22}(r_{ij}) \tag{13}$$

where

$$\psi_1(\lambda) = \sum_{i=1}^{N} u_{12}(r_{i,N+1};\ \lambda) \tag{14}$$

$$u_{12}(r;\ \lambda) = 4\lambda\epsilon_{12}\left[\left(\frac{\lambda\sigma_{12}}{r}\right)^{12} - \left(\frac{\lambda\sigma_{12}}{r}\right)^{6}\right] \tag{15}$$

$$u_{22}(r) = 4\epsilon_{22}\left[\left(\frac{\sigma_{22}}{r}\right)^{12} - \left(\frac{\sigma_{22}}{r}\right)^{6}\right] \tag{16}$$

Thus, $\psi_1(\lambda)$ is the potential energy of a solute molecule interacting with Lennard-Jones parameters given by:

$$\epsilon_\lambda = \lambda\epsilon_{12} \tag{17}$$

$$\sigma_\lambda = \lambda\sigma_{12} \tag{18}$$

Therefore, from Eq. 13, $u_{\lambda=1} = u_{\rm I}$ and $u_{\lambda=0} = u_{\rm II}$. Thus, the states II and I are smoothly connected through the parameter λ. The free energy between states defined at both λ' and λ is given by

$$\Delta A^r_\lambda = -kT\ln\langle\exp[\beta(u_{\lambda'} - u_\lambda)]\rangle_\lambda \tag{19}$$

where $\lambda' - \lambda$ is a small quantity so that $u_{\lambda'} - u_\lambda$ is of the order of kT. The chemical potential is obtained by taking the sum of these averages as follows:

$$\mu^r_1 = \sum_{\lambda=0}^{\lambda=1} \Delta A^r_\lambda \tag{20}$$

The perturbation method chemical potential expression in Eq. 20 is reminiscent of the Kirkwood coupling method. The two methods are related, and they become the same in the limit $\Delta\lambda \to 0$. This is easier to see when we write the Kirkwood chemical potential equation as:

$$\mu^r_1 = \int_0^1 \frac{dA^r}{d\lambda}\, d\lambda \tag{21}$$

where

$$A^r(\lambda) = -kT\ln\int \exp[-\beta u_\lambda]\, dr^{N+1} \tag{22}$$

with u_λ given in Eq. 13. Equation 22 gives the residual Helmholtz energy of the system as a function of the coupling parameter λ. It is clear that Eq. 21 is the differential limit of Eq. 20. Using Eq. 22 in Eq. 21 one can arrive at the familiar form of the Kirkwood chemical potential equation:

$$\mu^r_1 = 4\pi\rho\int_0^1\int_0^\infty \frac{du_{12}(r;\ \lambda)}{d\lambda} g_{12}(r;\ \lambda) r^2 dr d\lambda \tag{23}$$

where $g_{12}(r;\ \lambda)$ is the radial distribution function of solvent molecules around a solute molecule coupled to the extent λ to the rest of the system. In this work, we chose to use the perturbation approach, because it does not require quadrature at the end of the simulations and its implementation is quite straightforward.

Simulation Procedures

The simulations were carried out for the interconversion between an empty site and a solute molecule in the solution. A coupling parameter λ was used to smoothly transform the empty site ($\lambda = 0.0$), with $\epsilon = 0.0$ and $\sigma = 0.0$ Å, to solute molecule ($\lambda = 1.0$). Simulations were mainly carried out for values of $\lambda = 0.0$, 0.2, 0.4, 0.6, 0.8 and 1.0. In order to check the self-consistency of the calculations, the simulations were run in both directions, that is, $\lambda' \to \lambda$ and $\lambda \to \lambda'$ except at the two end points. This is known as "double-ended" sampling (Jorgensen and Ravimohan, 1985) and provides a measure of the accuracy in the calculations. In principle, the double-ended method is able to set both upper and lower bounds on the values obtained from the calculations. This bound, based upon the Gibbs-Bogoliubov-Feynmann inequality, was derived by Bennett (1976) and can be stated in the terms used here as:

$$-kT\ln\langle\exp[-\beta(u_{\rm I} - u_{\rm II})]\rangle_{\rm I} \le \mu^r_1 \le -kT\ln\langle\exp[-\beta(u_{\rm I} - u_{\rm II})]\rangle_{\rm II} \tag{24}$$

Using this inequality, one can estimate the range of accuracy of the calculations.

The simulations were done in the NVT ensemble. Throughout this work, we consider the near-critical region to be in the reduced variable ranges $T^* = 1.32 \pm 0.03$, $\rho^* = 0.30 \pm 0.02$. Three sampling systems were used as required, involving 124, 342 and 728 solvent molecules respectively. An attempt to move the solute was made on every 50th cycle of moving 124 solvents which was equal to every 6,200th configuration. The ranges for the attempted moves were almost the same in each simulation and provided approximately a 45% probability for the new configuration being accepted. For the system with one solute plus 124 solvent molecules, each simulation included an equilibrium phase of 100,000 configurations followed by averaging for properties over an additional 400,000 configurations *at each value of the perturbation parameter*. For the system with 342 solvent molecules, each simulation consisted of an equilibrium phase of 300,000 configurations; while for 728 solvent molecules, the equilibration phase was for 700,000 configurations. For the system of 124 solvent molecules, there was no statistically significant change in the computed chemical potential after averaging over these 400,000 configurations, while for the system of 342 solvent molecules, there was no significant change after 1,200,000 configurations. These numbers are the number of sampling steps at each value of λ throughout the respective simulation. For the Lennard-Jones energy functions, the recommended spherical cutoff distance $r_{\rm cutoff}$ is $2.5\sigma_{ij}$ (Allen and Tildesley, 1987). At this point the value of the pair potential between molecules i and j is just 1.6% of the well depth ϵ_{ij} and this value was used in this work.

Results and Discussion

In order to initially establish the merits of the free-energy perturbation algorithm as implemented here for the calculation of the infinite-dilution solute residual chemical potential μ^r_1, a comparison between our simulation results with some previously published work was done. In Table 2, we provide some of these results compared to those developed using both the test particle method and/or the Kirkwood coupling approach

Table 2. Reduced Infinite-Dilute Chemical Potential ($\mu_1'^* = \mu_1'/\epsilon_{22}$): Free-Energy Perturbation Method vs. Previous Literature Values

	$\epsilon_{12}=1.5\epsilon_{22}$, $\sigma_{12}^3=3.5\sigma_{22}^3$ and $T^*=2.0$	
ρ^*	Simulation Results (this work)	Literature Value
0.2	-7.33 ± 0.70	-7.4 ± 0.5*
0.4	-11.62 ± 1.59	-11.1 ± 0.5*
0.6	-6.32 ± 4.91	-10.0 ± 1.2**
	$\epsilon_{12}=2.0\epsilon_{22}$, $\sigma_{12}^3=3.5\sigma_{22}^3$ and $T^*=1.5$	
ρ^*	Simulation Results (this work)	Literature Value
0.1	-8.44 ± 0.63	-8.51†
0.2	-15.33 ± 1.02	-15.20†
0.3	-24.82 ± 1.84	-20.90†
0.4	-24.83 ± 1.82	-25.00†
0.5	-27.20 ± 4.31	-28.00†
0.6	-23.95 ± 5.22 -22.51 ± 1.15‡	-14.80†

*Using the test particle method by Shing and Chung (1988). For the test particle, the particle insertion simulation is considered more accurate than the particle withdrawal one (Shing and Gubbins, 1982).
**Using the Kirkwood coupling method by Shing and Chung (1988).
†Using the test particle method by Shing et al. (1988).
‡The simulation was run for values of $\lambda=0.0$, 0.1, 0.2, ..., 0.8, 0.9, and 1.0, and for the average over 1.0E6 configurations.

presented by Shing and co-workers. There is generally good agreement between our results and the prior work, with the only significant discrepancies occurring at the highest densities, particularly for the second system. To check this result, we repeated the simulation at the highest density for the second case in Table 2 for the smaller values of the perturbation parameter $\lambda=0.0$, 0.1, 0.2, ... 1.0. This halving of the perturbation step size results in a more accurate simulation; however, the change in the result we obtained was moderate suggesting that the test particle result may be suspect at this high density. These benchmarks showed that our simulations appeared to be accurate at the given conditions. However, it should be pointed out that the temperatures in Table 2 are all well removed from critical. We were unable to find published simulation results at conditions closer to the solvent critical point with which to compare our calculations so in subsequent sections we have compared the simulations to theoretical results where possible. This theory used the Kirkwood-Buff formalism in conjunction with the Percus-Yevick model for the various solution pair correlation functions. Notwithstanding this being a classical theory, in previous work when compared to simulation results in supercritical fluid systems at conditions more remote from critical than those investigated here, it has acquitted itself quite well (McGuigan and Monson, 1990). Since this theory implicitly accesses long-range structure, any strong discrepancies between the simulation results and theory can serve as a *useful guide* to potential size dependence problems with the simulations; this perspective was particularly useful for analyzing the results as now discussed.

In Figure 1 and Table 3, results are provided showing the values of μ_1' calculated over a wide range of densities at a temperature much closer to the critical one, that is $T^*=1.32$. In addition, we also show the integral equation results for μ_1' at similar conditions. The agreement between both sets of numbers is quite good, particularly at the lowest densities where we are more confident of the theory. In general, the integral equation results tend to fall within the range of the inequality given by Eq. 24 especially for the simulations at the smallest value of $\Delta\lambda$. The simulations for $\Delta\lambda=0.1$ are modestly different from those at twice the value of this perturbation step size; the largest differences occur as expected at the highest densities. At these high densities, there is generally greater uncertainty to the simulation results as indicated by the increasing range of the "double-ended" sampling calculations representing the range of the inequality given by Eq. 24. This degradation in simulation results at high densities corresponds to the difficulty of finding accessible regions of phase space in which to move the system's molecules when they are closely packed. It is of interest to note that the result closest to the critical point shows extremely good agreement between theory and simulation values for μ_1'. Since the theory implicitly incorporates long-range effects, while the simulations by construction do not, this reinforces the earlier result that μ_1' is largely independent of long-range structure at near-critical conditions.

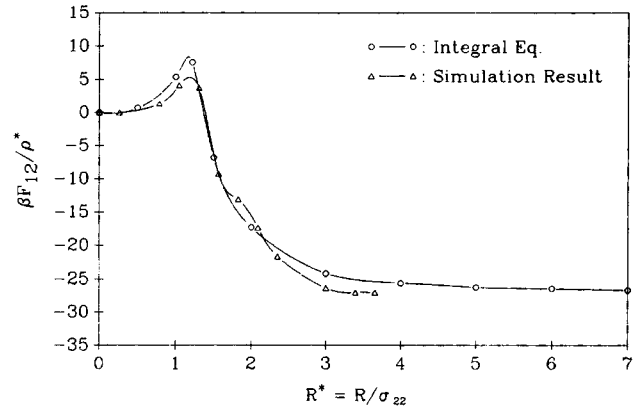

Figure 1. Comparison of the residual chemical potential μ_1' by MC simulations and integral equation theory calculations where $T^*=1.32$.

Sample size and simulation results for μ_1'

In order to further test the integrity of the simulation results, we explicitly addressed the question of system size and its effect on the results. Although μ_1' may primarily be given by short-range effects, this *does not* entirely absolve simulation methods from having to deal with the question of long-range fluctuations that are present near the solvent critical point. The reason for this is that while the final equilibrium value for μ_1' may depend mainly on molecular configurations within a small neighborhood around the solute species, these configurations must be allowed to occur during the simulation, and this process may indeed involve large length scale fluctuations. In other words, the system size in the NVT ensemble may yet be an important factor determining the extent to which molecules at a significant distance from the solute will be allowed to be drawn into the local neighborhood that determines the value of the property μ_1'. We investigated this issue using systems of various size.

Table 4 shows results illustrating this very close to the solvent critical point. Different systems corresponding to $N_2=124$, $N_2=342$ and $N_2=728$ were used to determine μ_1'. The results show that increasing the number of solvent molecules in the simulations did not have a very significant effect on the simulation results for the ensemble average for μ_1'. From these and other similar results, we have found it appears that system size

Table 3. Residual Chemical Potential Values found by MC Simulation and Integral Equation Theory*

ρ^*	Computer Simulation ($N_2=124$) μ_1^r (kcal/mol) $\lambda=0.0, 0.2 \ldots 0.8$ and 1.0	Computer Simulation ($N_2=124$) μ_1^r (kcal/mol) $\lambda=0.0, 0.1 \ldots 0.9$ and 1.0	Theory** μ_1^r (kcal/mol)
0.05	II→I: −0.84 I→II: 0.96 ⟩ −0.90⟩		−0.84
0.1	II→I: −1.69 I→II: 1.75 ⟩ −1.72⟩	II→I: −1.63 I→II: 1.71 ⟩ −1.67⟩	−1.67
0.2	II→I: −3.05 I→II: 3.24 ⟩ −3.15⟩	II→I: −2.94 I→II: 3.10 ⟩ −3.02⟩	−3.25
0.3	II→I: −4.21 I→II: 4.73 ⟩ −4.47⟩	II→I: −4.06 I→II: 4.45 ⟩ −4.25⟩†	−4.33
0.4	II→I: −5.04 I→II: 5.45 ⟩ −5.25⟩	II→I: −4.83 I→II: 5.29 ⟩ −5.06⟩†	−4.85
0.5	II→I: −5.77 I→II: 6.20 ⟩ −5.99⟩	II→I: −5.19 I→II: 5.36 ⟩ −5.28⟩†	−5.41
0.6	II→I: −5.88 I→II: 7.19 ⟩ −6.54⟩	II→I: −5.59 I→II: 6.65 ⟩ −6.12⟩†	−5.80

* State I means the system has N_2 solvent molecules and 1 solute; state II means the system has only N_2 solvent molecules: $T^*=kT/\epsilon_{22}=1.32$. Here, μ_1^r of II→I is calculated by the equation $(-RT\ln\langle e^{-\beta\Delta u}\rangle_{II})$ and μ_1^R of I→II is calculated by $(-RT\ln\langle e^{-\beta\Delta u}\rangle_{I})$. Numbers inside ⟨ ⟩ are the average of $(-RT\ln\langle e^{-\beta\Delta u}\rangle_{II})$ and $(-RT\ln\langle e^{-\beta\Delta u}\rangle_{I})$.
* Please see reference Munoz and Chimowitz (1992).
** The simulations were run for the average over 1.0E6 configurations.

does not appear to play a significant role in determining μ_1^r, at least for the potentials studied. Because of the long computer times involved with the calculations using $N_2=728$ solvent molecules, we only did these calculations for $\Delta\lambda=0.2$. These results, as well as the others in Table 4, clearly demonstrate the small effects of size dependence on μ_1^r. In Figure 2 are shown values for μ_1^r plotted at intermediate stages during the simulation showing the convergence characteristics of these simulation runs at the conditions shown.

Local density enhancements and simulation of other properties

The enhancement of solvent density in the immediate neighborhood of the solute relative to the prevailing bulk fluid density has interested a number of research groups in supercritical fluid solution thermodynamics (Kim and Johnston, 1987; Debenedetti and Kumar, 1988; Munoz and Chimowitz, 1992). The results in Table 5 show the local density enhancements in a region corresponding to three solvent diameters around the solute, calculated both with simulations and theory. The local density factor $\Delta\rho_{loc}$ is defined as:

$$\Delta\rho_{loc}=\left(\frac{N-N_v}{N_v}\right)\times 100\% \tag{25}$$

where N is the actual number of molecules in the local volume defined as:

$$N=\rho\int_0^{3\sigma_{22}} g_{12}(r)\,4\pi r^2 dr \tag{26}$$

Table 4. Residual Chemical Potential Values Found by MC Simulation Using 125 Particles ($N_2=124$ and $N_1=1$), 343 Particles ($N_2=342$ and $N_1=1$) and 729 Particles ($N_2=728$ and $N_1=1$)*

	$N_2=124$ (MC Simulation)	$N_2=342$ (MC Simulation)	$N_2=729$ (MC Simulation)	Theory**
μ_1^r (kcal/mol) where $\Delta\lambda=0.2$	−4.47±0.26	−4.68±0.15	−4.52±0.01	−4.33
μ_1^r (kcal/mol) where $\Delta\lambda=0.1$	−4.25±0.20	−4.35±0.15	——	−4.33

* State I means the system has N_2 solvent molecules and 1 solute; state II means the system has only N_2 solvent molecules: $T^*=kT/\epsilon_{22}=1.32$, $\rho^*=0.3$
** Please see reference Munoz and Chimowitz (1992).

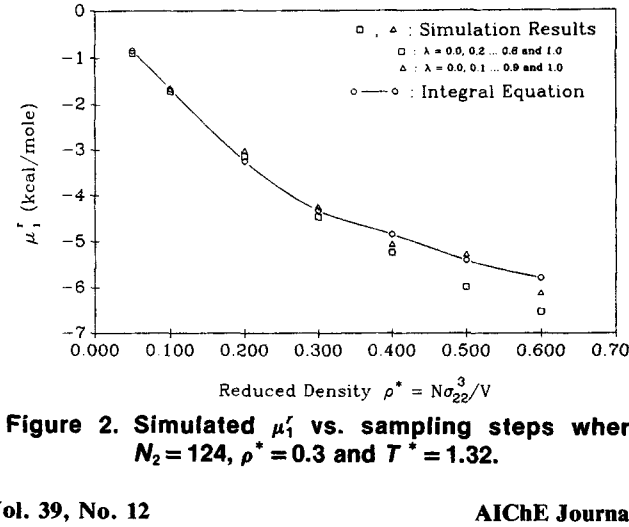

Figure 2. Simulated μ_1^r vs. sampling steps where $N_2=124$, $\rho^*=0.3$ and $T^*=1.32$.

Table 5. u_1 (Average Potential Energy of Solute), N (Number of *Local* Solvent Molecules) and $\Delta\rho_{loc}$ (Local Density Enhancement Factor) Calculated by MC Simulations and Integral Equation Theory*

	Simulation ($N_2=124$)	Theory**	Simulation ($N_2=124$)	Theory	Simulation ($N_2=124$)	Theory
ρ^*	u_1 (kcal/mol)	u_1 (kcal/mol)	N	N	$\Delta\rho_{loc}$	$\Delta\rho_{loc}$
0.05	−1.53	−1.51	7.51	7.43	38.46%	36.88%
0.1	−2.86	−3.06	14.30	15.62	31.75%	43.93%
0.2	−5.05	−6.59	27.05	35.16	24.64%	62.04%
0.3	−6.62	−8.70	37.19	49.00	14.24%	50.53%
0.4	−7.90	−8.69	46.88	50.89	8.00%	17.25%
0.5	−8.98	−9.64	56.33	57.94	3.82%	6.80%
0.6	−10.33	−10.99	66.08	67.09	3.03%	3.05%

* Total sampling steps for simulations are 1,000,000 and $T^* = kT/\epsilon_{22} = 1.32$
** Please see reference Munoz and Chimowitz (1992)

and N_v is the number of molecules in this volume element that would exist if the local density were equal to the prevailing bulk density ρ_v. In addition, in Table 5 are shown the results for u_1, the local energetic contribution to μ_1^r, defined in Eq. 3. At both very low and high densities, there is good agreement between theory and simulation for u_1, N and $\Delta\rho_{loc}$, but at intermediate densities, especially near the critical point, there are significant discrepancies between these values. Obviously for *these* properties, the existence of long-range fluctuations near the critical point seems to be a factor that may be inadequately accounted for using the sample size corresponding to $N_2 = 124$. These observations motivated us to study the issue of the sample size for these respective properties. Simulations were done using $N_2 = 124$, 342 and 728, the results of which are presented in Table 6. The change in the results with increasing sample size is clear, showing the salutary effects of increasing both system size (and the number of sampling steps) for these respective properties. It is interesting to note that at the high end of the simulations ($N_2 = 728$, number of sampling steps = 7.0E6) the simulations appear to be converging toward the results given by theory. Presumably, the results of this trend could be made more accurate by continuing to increase both N_2 and the sampling steps of the MC algorithm.

These results illustrate a number of issues related to MC simulations near the solvent critical point. They show that a property like μ_1^r appears to not require very large sample sizes while other properties like u_1, $\Delta\rho_{loc}$ and so on appear to be significantly improved as sample size increases. Although all three of these properties are in the final analysis primarily

Table 6. u_1 (Average Potential Energy of Solute), N (Number of Local Solvent Molecules) and $\Delta\rho_{loc}$ (Local Density Enhancement Factor) Calculated by Sampling 125 Particles ($N_2 = 124$ and $N_1 = 1$), 343 Particles ($N_2 = 342$ and $N_1 = 1$) and 729 Particles ($N_2 = 728$ and $N_1 = 1$) with Different Sampling Steps*

	$N_2=124$	$N_2=342$	$N_2=728$	Theory**
u_1 (kcal/mol)	$-6.63^{(1.0E6)}$	$-7.80^{(3.0E6)}$	$-7.89^{(7.0E6)}$	−8.70
N	37.19	43.84	45.31	49.00
$\Delta\rho_{loc}$	14.24%	34.68%	39.18%	50.53%

* $T^* = kT/\epsilon_{22} = 1.32$, $\rho^* = 0.3$
** From Munoz and Chimowitz (1992).

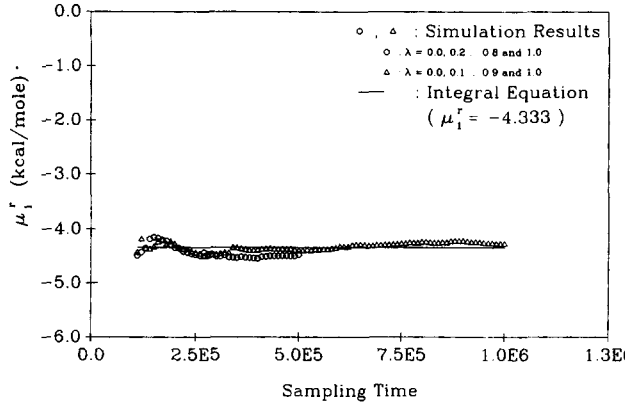

Figure 3. $\beta F_{12}/\rho^*$ at $T^* = 1.32$ and $\rho^* = 0.3$.

given by short-range structure, it is clear that the 'correct' local structure of the fluid requires that long-range effects be free to influence the progression towards the 'final' equilibrium state. If this is restricted in the simulations, by arbitrarily reducing the sample size for example, then considerable errors may occur. We emphasize though *that μ_1^r remains relatively insensitive to the values of local density enhancements* as may be inferred from the results in Tables 4 and 6, consistent with the theoretical analysis of Munoz and Chimowitz (1992). This invariance was attributed to short-range energy-entropy cancellation effects as borne out by the simulations. On the other hand a property like u_1, although also dependent on short-range structure, is more strongly dependent upon density enhancements in the immediate neighborhood of the solute.

Figure 3 shows a comparison between theory and simulation results illustrating the spatial dependence of μ_1^r, represented by the function $F_{12}(R)$ defined in Eq. 7. Each simulation point in Figure 3 represents the simulation result analogue of Eq. 7 at a given distance $R^* = R/\sigma_{22}$ from the solute molecule. To get these results the simulations were done such that the cutoff distance for the solute molecule *was made equal to R^* for each respective simulation point on the graph*. The results are for a condition very close to the solvent critical point and indicate a reassuring consistency between theory and simulation at this level of molecular detail.

Given these results for pure solvent systems in their near-critical regions we decided to simulate near-critical mixed solvent systems for the final results of this article. To our best knowledge, such calculations close to the solvent mixture's critical point have not previously been reported.

Mixture simulations

An advantage of computer simulation is its flexibility for addressing variations of a problem without having to radically reformulate equations and other theoretical results. To this end, we chose to study a fluid solvent mixture near its critical region. Supercritical fluid solvent mixtures exhibit a variety of interesting behavior including the phenomenon referred to as critical azeotropy, a topic discussed in detail by Munoz and Chimowitz (1993a,b). The fluid mixture we investigated was represented by Lennard-Jones potential parameters shown in Table 7 for components 2 and 3, for which Munoz (1992) has provided critical line results using integral equation theory calculations. The results for the critical line of this binary

Table 7. Lennard-Jones Potential Parameters for the Mixed Near-Critical Solvent System

	ϵ_{ij}/k (K)	σ_{ij} (Å)
Solute 1-Solute 1	307.02	4.374
Solvent 2-Solvent 2	409.36	4.918
Solvent 3-Solvent 3	204.68	3.831
Solute 1-Solvent 2	354.52	4.647
Solute 1-Solvent 3	250.68	4.103
Solvent 2-Solvent 3	289.46	4.375

mixture are presented in Figure 4. We were interested in examining the chemical potential of a third dilute solute species, with potential parameters shown in Table 7, immersed in the mixed fluid solvent system at various reduced conditions of temperature and density. These reduced variables were defined as $T_r = T/T_c$ and $\rho_r = \rho/\rho_c$, where T_c and ρ_c refer to the absolute critical temperature and density of the solvent phase respectively, which can be found from Figure 4. The results for the solute residual chemical potential are shown in Figure 5. It should be noted that the 1-2 solute-solvent system's residual chemical potential lies above the values for the 1-3 pair. Table 7 shows that the potential parameters for the 1-2 pair reflects a more 'positive' solution, that is, solute molecule 'smaller' than the solvent while the 1-3 pair is a more 'attractive' solution (solute larger than the solvent species). These results are completely consistent with the integral equation results of our earlier work, Munoz and Chimowitz (1992), for these types of solutions. This ordering relationship between these two classes of solutions can also be understood from Eq. 1 where the integrand shows that the more positive a solution, the lower the respective values for the pair correlation function at a given intermolecular separation and hence the higher the values for μ_1^r expected at a given reduced density. The minimum in μ_1^r for the 1-2 solution that may be inferred from Figure 5 at higher densities is also consistent with the integral equation calculations and is in keeping with the decrease in solubility at high solvent densities that has been discussed by Kurnik and Reid (1981). Also shown in Figure 5 are results for a solvent mixture with $x_2 = 0.508$. It is evident that the mixture values lie intermediate to those of the respective pure solvents at similar

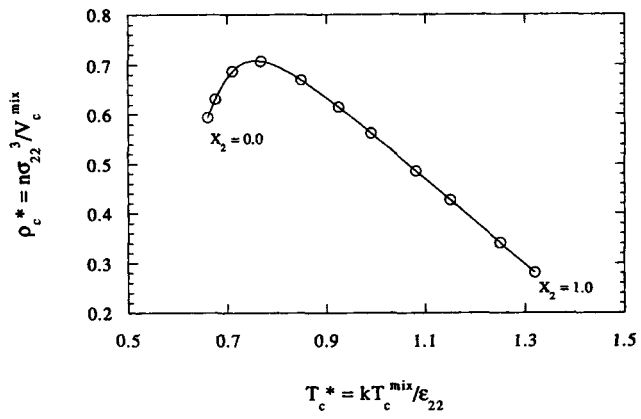

Figure 4. Critical locus (temperature vs. density) of a liquid mixture represented by solvent 2 and solvent 3 in Table 7.

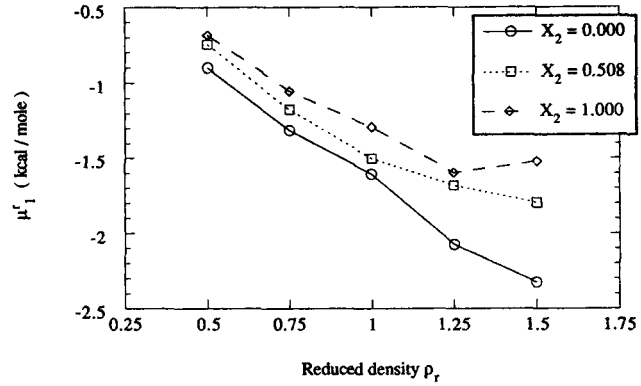

Figure 5. Residual chemical potential μ_1^r vs. reduced density ρ_r for various near-critical solvent mixtures where $T_r = 1.05$.

conditions of T_r and ρ_r. These results are representative of others that we have found with various solvent mixture compositions and indicate no untoward behavior of the fluid mixture as solvent. We also took this opportunity to evaluate a well-known approximate theory for fluid mixtures, namely the van der Waals one fluid (VDW1) model (Leland et al., 1968; Henderson and Leonard, 1971; MacGowan et al., 1985). In this regard, we treated the 1,2 solvent mixtures as a 'synthetic' one fluid with fluid properties given by the established VDW1 mixing rules for the potential parameters,

$$\epsilon_x \sigma_x^3 = \sum_i \sum_j x_i x_j \epsilon_{ij} \sigma_{ij}^3 \tag{27}$$

$$\sigma_x^3 = \sum_i \sum_j x_i x_j \sigma_{ij}^3 \tag{28}$$

where ϵ_x and σ_x are the one fluid well depth and size parameters, respectively. The purpose of the computations was to evaluate the solute residual chemical potential μ_1^r in this synthetic VDW1 fluid solvent and compare the results with the simulation results of the actual fluid mixture which we term the exact results. These comparisons are shown in Figures 6 and 7 for two different mixture compositions studied by Munoz (1992) with critical parameters, as shown in Table 8. The agreement be-

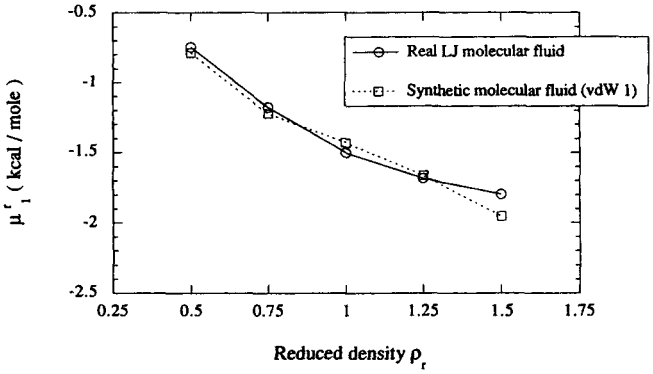

Figure 6. Residual chemical potential μ_1^r vs. reduced density ρ_r for $x_2 = 0.508$ where $T_r = 1.05$.

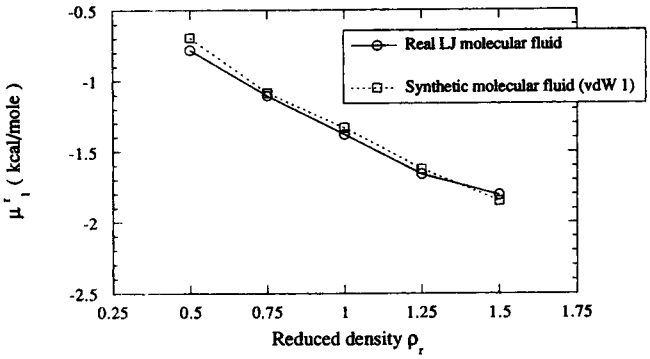

Figure 7. Residual chemical potential μ_1^r vs. reduced density ρ_r for $x_2 = 0.75$ where $T_r = 1.05$.

tween the approximate theory and the exact results, at least for the property μ_1^r, is impressive and represents a success for the VDW1 theory for this new series of calculations.

Conclusions

The purpose of this article has been to address several issues associated with computer simulation of dilute mixture thermodynamic properties at conditions close to the system's critical point. A number of questions arise in these circumstances because of the potentially contradictory demands of the problem being studied. On the one hand, simulations usually involve the use of relatively small system sizes for the calculations, while on the other hand critical phenomena related to second-order phase transitions implicitly involve long length scale intermolecular correlations. Can these two situations be reconciled so that the simulations provide useful information?

The results here demonstrate that for properties like the solute chemical potential, this conflict can be successfully overcome largely because of the inherently short-range nature of this particular property, as well as the fact that it is insensitive to local solvent density enhancements even when the local density values depart significantly from bulk ones. The energy-entropy cancellation effect that accounts for the relative insensitivity of μ_1^r to local solvent density enhancement, has been borne out by the results and confirms our previous results obtained using integral equation theory calculations. At conditions very close to the critical point, tripling sample size did not significantly affect the simulation results for μ_1^r although tripling the number of simulation steps did increase accuracy, as might be expected. These calculations were all done in the NVT ensemble which has sometimes been held open to question for use in simulations of near-critical systems; the reason for this being that at the outset of the simulation the ensemble density is fixed, and it is felt that this might suppress the effects of local density fluctuations to the detriment of the calculations. This does not appear to be necessarily the case based upon the results provided here. On the other hand, properties like u_1 (average configurational energy of a solute molecule) were examined and appeared to be more strongly affected by the ensemble size used—the larger the sample size, the more accurate were the results found. Clearly, simulation requirements for different classes of properties in near-critical mixtures will vary, dependent upon the sensitivity of long-range effects to the property in question. When these effects are relevant to the property in question, accuracy in the simulations will require careful attention to the size of the system and other algorithmic details.

An important role of computer simulation is to provide benchmark results for fluid thermodynamics properties against which to test approximate physical theories. These theories usually arise as a consequence of having to simplify the mathematical form of the exact expressions given by rigorous statistical mechanics. Here we evaluated such a theory in comparison with simulation results for the solute chemical potential in a supercritical fluid solvent. While some comparisons have previously been made between this theory and simulation results, these have generally not been at the critical point or in its close vicinity like the results presented here. For the solute chemical potential at conditions investigated in this article, the agreement between theory and the most accurate simulations has often been very good, suggesting that the theory captures many of the important effects describing near-critical fluid behavior. Finally, we compared mixture results obtained from simulations with a well-known approximate theory for fluid mixture properties and once again agreement between theory and simulation was shown to be quite good.

Table 8. Thermodynamic Properties of Near-Critical Solvent Mixtures*

System	A	B	C	D
x_2	0.00	0.51	0.75	1.00
N_2	0	63	93	124
T_c(K)	270.112	470.764	511.700	540.224
ρ_c(mol/cm^3)	8.323E-3	5.982E-3	4.776E-3	3.935E-3
ϵ_x/k(K)	204.68	306.25	356.48	409.36
σ_x(Å)	3.831	4.383	4.646	4.918

*x_2 is the mole fraction of solvent 2, N_2 is the number of molecules of solvent 2 in the sampling box, T_c and ρ_c are critical temperatures and densities for various solvent mixtures, and ϵ_x/k and σ_x are the LJ parameters provided by the van der Waals one fluid theory.

Acknowledgment

The authors would like to acknowledge the National Science Foundation for partial financial support of this work through grant No. CBT-9213276. In addition, this research was conducted using the resources of Cornell Research Center which receives funding from NSF, IBM Corp., and New York State Science and Technology Foundation.

Notation

A^r = residual Helmholtz free energy
$F_{12}(R)$ = spatial function of μ_1^r
$g(r, \xi)$ = molecular pair correlation function
$\bar{H}_1^r$ = residual partial molar enthalpy of the solute
I = thermodynamic state of solution including N_2 solvent with 1 solute
II = thermodynamic state of solution including N_2 solvent only
k = Boltzmann's constant
L = length of a sampling box
N = actual number of molecules
N_v = existing number if local density equals prevailing bulk density
r = intermolecular distance
$\bar{S}_1^r$ = residual partial molar entropy of the solute
T = temperature
T^* = reduced temperature with respect to energy wall depth of LJ parameter ($=kT/\epsilon_{22}$)
T_c^{mix} = critical temperature of liquid mixture

T_r = reduced temperature with respect to critical temperature of liquid mixture ($=T/T_c^{mix}$)
u_1 = average potential energy of solute
$\overline{U}_1^{\infty}$ = solute partial molar internal energy at infinite-dilution solution
V = volume
V_c^{mix} = critical volume of liquid mixture
$\overline{V}_1^{\infty}$ = solute partial molar volume at infinite-dilution solution
1 = solute molecule
2 = solvent molecule
3 = solvent molecule

Greek letters

β = $1/kT$
ϵ = well-depth parameter of Lennard-Jones energy function
λ = perturbation parameter
μ_1^r = solute residual chemical potential
ξ = Kirkwood coupling parameter
ρ = density ($=N/V$)
$\Delta\rho_{loc}$ = local density enhancement
ρ_c^{mix} = critical density of liquid mixture ($=N/V_c^{mix}$)
ρ^* = reduced density with respect to collision diameter ($=N\sigma_{22}^3/V$)
ρ_r = reduced density with respect to critical density of liquid mixture ($=N/V_c^{mix}$)
σ = collision diameter of Lennard-Jones energy function

Literature Cited

Allen, M. P., and D. J. Tildesley, *Computer Simulation of Liquids*, Oxford Science Publications (1987).

Bennett, C. H., "Efficient Estimation of Free Energy Differences from Monte Carlo Data," *J. Comput. Phys.*, **22**, 245 (1976).

Debenedetti, P. G., and S. K. Kumar, "The Molecular Basis of Temperature Effects in Supercritical Extraction," *AIChE J.*, **34**, 645 (1988).

Henderson, D., and P. J. Leonard, "Liquid Mixtures," *Physical Chemistry—An Advanced Treatise*, **8B**, 414 (1971).

Jorgensen, W. L., and C. Ravimohan, "Monte Carlo Simulation of Differences in Free Energies of Hydration," *J. Chem. Phys.*, **83**, 3050 (1985).

Kim, S. W., and K. P. Johnston, "Molecular Interactions in Dilute Supercritical Fluid Solutions," *Ind. Eng. Chem. Res.*, **26**, 1206 (1987).

Kirkwood, J. G., and F. P. Buff, "The Statistical Mechanical Theory of Solutions: I," *J. Chem. Phys.*, **19**, 774 (1951).

Kurnik, R. T., and R. C. Reid, "Solubility Extrema in Solid-Fluid Equilibria," *AIChE J.*, **27**, 861 (1968).

Leland, T. W., J. S. Rowlinson, and G. A. Sather, "Statistical Thermodynamics of Mixtures of Molecules of Different Sizes," *Trans. Faraday Soc.*, **64**, 1447 (1968).

MacGowan, D., J. L. Lebowitz, and E. M. Waisman, "Van der Waals One-fluid Theory: Justification and Generalization," *Fluid Phase Equilibria*, **57**, 227 (1990).

McGuigan, D. B., and P. A. Monson, "Analysis of Infinite Dilution Partial Molar Volumes Using a Distribution Function Theory," *Fluid Phase Equilib.*, **57**, 227 (1990).

McQuarrie, D. A., *Statistical Mechanics*, Harper & Row, New York (1973).

Munoz, F., and E. H. Chimowitz, "Integral Equation Calculations of the Solute Chemical Potential in a Near-critical Fluid Environment," *Fluid Phase Equilib.*, **71**, 237 (1992).

Munoz, F., and E. H. Chimowitz, "Critical Phenomena in Fluid Mixtures: I. Thermodynamic Theory for the Binary Critical Azeotrope," *J. Chem. Phys.*, **99**, 5438 (1993a).

Munoz, F., and E. H. Chimowitz, "Critical Phenomena in Fluid Mixtures: II. Synergistic and Other Effects Near Mixture Critical Points," *J. Chem. Phys.*, **99**, 5450 (1993b).

Munoz, F., "The Statistical Mechanics of Solutions Near a Critical Point Phase Transition," PhD Diss., Univ. of Rochester, Rochester, New York (1992).

Nouacer, M., and K. S. Shing, "Grand Canonical Monte Carlo Simulation for Solubility Calculation in Supercritical Extraction," *Mol. Sim.*, **2**, 55 (1989).

Panagiotopoulos, A. Z., U. W. Suter, and R. C. Reid, "Phase Diagrams of Nonideal Fluid Mixtures from Monte Carlo Simulation," *Ind. Eng. Chem. Fundam.*, **25**, 525 (1986).

Petsche, I. B., and P. G. Debenedetti, "Solute-solvent Interactions in Infinitely Diluted Supercritical Mixtures: A Molecular Dynamics Investigation," *J. Chem. Phy.*, **91**, 7075 (1989).

Percus, J. K., and G. K. Yevick, "Analysis of Classical Statistical Mechanics by Means of Collective Coordinates," *Phys. Rev.*, **110**, 1 (1958).

Shing, K. S., and S. T. Chung, "Computer Simulation Methods for the Calculation of Solubility in Supercritical Extraction Systems," *J. Phys. Chem.*, **91**, 1674 (1987).

Shing, K. S., and S. T. Chung, "Calculation of Infinite-dilution Partial Molar Properties by Computer Simulation," *AIChE J.*, **34**, 1973 (1988).

Shing, K. S., and K. E. Gubbins, "The Chemical Potential From Computer Simulation Test Particle Method with Umbrella Sampling," *Molec. Phys.*, **43**, 717 (1981).

Shing, K. S., and K. E. Gubbins, "The Chemical Potential in Dense Fluids and Fluid Mixtures via Computer Simulation," *Molec. Phys.*, **46**, 1109 (1982).

Shing, K. S., K. E. Gubbins, and K. Lucas, "Henry Constants in Non-ideal Fluid Mixtures. Computer Simulation and Theory," *Molec. Phys.*, **65**, 1235 (1988).

Singh, U. C., F. K. Brown, P. A. Bash, and P. A. Kollman, "An Approach to the Application of Free Energy Perturbation Methods Using Molecular Dynamics: Applications to the Transformations of $CH_3OH \rightarrow CH_3CH_3$, $H_3O^+ \rightarrow NH_4^+$, Glycine→Alanine, and Alanine→Phenylalanine in Aqueous Solution and to $H_3O^+(H_2O)_3 \rightarrow NH_4^+(H_2O)_3$ in the Gas Phase," *J. Am. Chem. Soc.*, **109**, 1607 (1987).

Vogelsang, R., and C. Hoheisel, "Structure and Dynamics of a Supercritical Fluid in Comparison with a Liquid. A Computer Simulation Study," *Molec. Phys.*, **53**, 1355 (1984).

Widom, B., "Some Topics in the Theory of Fluids," *J. Chem. Phys.*, **39**, 2808 (1963).

Wu, R., L. L. Lee, and H. D. Cochran, "Structure of Dilute Supercritical Solutions: Clustering of Solvent and Solute Molecules and the Thermodynamic Effects," *Ind. Eng. Chem. Res.*, **29**, 977 (1990).

Manuscript received Nov. 23, 1992, and revision received Apr. 19, 1993.